THE ASTROPHYSICAL JOURNAL, 595:L127–L130, 2003 October 1

REGULARIZED ELECTRON FLUX SPECTRA IN THE 2002 JULY 23 SOLAR FLARE

MICHELE PIANA,[1] ANNA MARIA MASSONE,[2] EDUARD P. KONTAR,[3,4] A. GORDON EMSLIE,[4]
JOHN C. BROWN,[3,4] AND RICHARD A. SCHWARTZ[5]
Received 2002 March 11; accepted 2003 May 15; published 2003 September 8

ABSTRACT

By inverting the *Reuven Ramaty High Energy Solar Spectroscopic Imager* (*RHESSI*) hard X-ray photon spectrum with the Tikhonov regularization algorithm, we infer the effective mean electron source spectrum for a time interval near the peak of the 2002 July 23 event. This inverse approach yields the smoothest electron flux spectrum consistent with the data while retaining real features, such as local minima, that cannot be found with forward model-fitting methods that involve only a few parameters. A significant dip in the recovered mean source electron spectrum near $E = 55$ keV is noted, and its significance briefly discussed.

Subject heading: Sun: flares

1. INTRODUCTION

As discussed by Brown, Emslie, & Kontar (2003), hard X-ray spectra $I(\epsilon)$ in solar flares can be used, in conjunction with a suitable bremsstrahlung cross section $Q(\epsilon, E)$, to determine the *effective mean electron flux spectrum* $F(E)$ in the source, viz.,

$$I(\epsilon) = \frac{1}{4\pi R^2}\,\bar{n}V\int_{\epsilon}^{\infty}\bar{F}(E)Q(\epsilon, E)dE, \tag{1}$$

where R is the distance to the observer and the mean target density $\bar{n} = V^{-1}\int n(\boldsymbol{r})dV$. The function $F(E)$ represents the density-weighted mean electron spectrum in the source and is "effective" in the sense that it is influenced by factors such as secondary (e.g., photospheric albedo) emission in the observed $I(\epsilon)$. It is a quantity that is obtained solely from the observed photon spectrum $I(\epsilon)$; it requires no assumptions about physical conditions (e.g., thin target vs. thick target, uniform vs. nonuniform) in the bremsstrahlung source (Brown et al. 2003).

The Volterra integral (eq. [1]) for $F(E)$ can be solved either by forward-fitting parameterized forms of $F(E)$ to $I(\epsilon)$ (e.g., Holman et al. 2003) or by direct inversion of the integral equation. Such an inversion may be performed by several equivalent methods, e.g., differentiation (possibly of fractional order; Brown 1971) or discretization followed by matrix inversion (Johns & Lin 1992). However, the ill-posed nature of the inverse problem (eq. [1]; e.g., Craig & Brown 1986) may result in a large amplification of data noise in the recovered $F(E)$. Thompson et al. (1992), Piana (1994), and Piana & Brown (1998) have therefore presented a *regularized* inversion algorithm that maintains much of the fidelity in the recovered $F(E)$, while effectively suppressing much of the noise amplification through the imposition of a degree of smoothness in the recovered solution (see, e.g., eq. [2]). The latter two of these works employ an approach based on the Tikhonov (1963) regularization algorithm, which utilizes the singular value decomposition (SVD) of a linear operator for its implementation (Golub & Van Loan 1933). In this Letter, we apply this Tikhonov regularization technique to deduce the form of $F(E)$ for a 20 s interval near the peak of the 2002 July 23 flare. Significant features in $F(E)$ not realizable through limited-parameter forward-fitting techniques (e.g., Holman et al. 2003) are indeed revealed.

2. DERIVATION OF REGULARIZED MEAN ELECTRON FLUX SPECTRA

The formal methodology of the Tikhonov (1963) regularization technique was first applied to high-resolution solar hard X-ray spectra by Piana (1994) and Piana & Brown (1998). Essentially, the method consists of writing equation (1) in the discretized matrix form $\boldsymbol{I} = \boldsymbol{A}\boldsymbol{F}$, where, in general, $\boldsymbol{I}$ is an M-vector representing the observed photon spectrum $I(\epsilon)$, A is an $M \times N$ matrix representing the cross section $Q(\epsilon, E)$, and $\boldsymbol{F}$ is an N-vector representing the mean electron spectrum $F(E)$. We seek the solution of the minimization problem

$$\left\|\boldsymbol{A}\bar{\boldsymbol{F}} - \boldsymbol{I}\right\|^2 + \lambda\left\|\bar{\boldsymbol{F}}\right\|^2 = \text{minimum}, \tag{2}$$

where the double bars denote the Euclidean norm of a vector and the regularization parameter λ tunes the trade-off between the fidelity of the data fit (measured by the first term on the left-hand side of eq. [2]) and the smoothness in the recovered $\boldsymbol{F}$ (measured by the second term). In order to compute the solution of the minimization problem (eq. [2]), we utilized the SVD of $\boldsymbol{A}$, namely, the set of triples $\{\sigma_k;\ \boldsymbol{v}_k, \boldsymbol{u}_k\}_{k=1}^{p}$, $p = \min(M, N)$, that satisfy the *shifted eigenvalue problem*

$$\boldsymbol{A}\boldsymbol{u}_k = \sigma_k\boldsymbol{v}_k; \quad \boldsymbol{A}^T\boldsymbol{v}_k = \sigma_k\boldsymbol{u}_k, \tag{3}$$

where $\boldsymbol{A}^T$ is the transpose of $\boldsymbol{A}$; $\boldsymbol{u}_k$ and $\boldsymbol{v}_k$ are eigenvectors of length N and M, respectively; and the eigenvalues σ_k are real positive numbers with $\sigma_1 \geq \sigma_2 \geq \ldots \geq \sigma_p$. It can be shown

[1] Istituto Nazionale di Fisica della Materia and Dipartimento di Matematica, Università di Genova, via Dodecaneso 35, I-16146 Genoa, Italy; piana@dima.unige.it.
[2] Istituto Nazionale di Fisica della Materia, Unità di Ricerca di Genova, via Dodecaneso 33, I-16146 Genova, Italy; massone@ge.infm.it.
[3] Department of Physics and Astronomy, University of Glasgow, The Kelvin Building, G12 8QQ, UK; eduard@astro.gla.ac.uk, john@astro.gla.ac.uk.
[4] Department of Physics, The University of Alabama in Huntsville, Huntsville, AL 35899; emslieg@uah.edu.
[5] Science Systems and Applications, Inc., Laboratory for Astronomy and Solar Physics, Code 682, NASA Goddard Space Flight Center, Greenbelt, MD 20771; richard.schwartz@gsfc.nasa.gov.

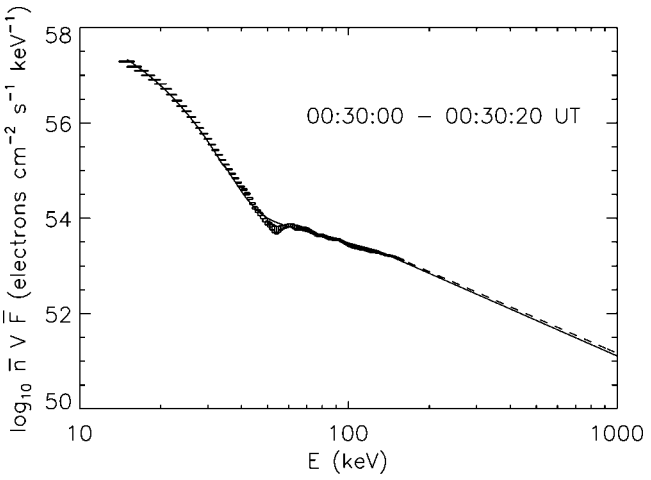

FIG. 1.—Regularized spectrum $\bar{n}V\bar{F}$ vs. E for the time interval 00:30:00–00:30:20 UT, obtained using the Haug (1997) cross section. The spectrum has been extended from 160 keV to 1 MeV using a power law of index $\delta = 2.45$ (*dashed line*; see text for details). The vertical sizes of the error boxes from $E = 15$ keV through $E = 160$ keV reflect the $3\,\sigma$ limits caused by statistical noise in the observed photon spectrum $I(\epsilon)$. The forward-fitted spectrum of Holman et al. (2003), using the same cross section, is shown as a solid line.

(Bertero, de Mol, & Pike 1988) that the formal solution of equation (2) is given by

$$\bar{\boldsymbol{F}} = \sum_{k=1}^{p} \frac{\sigma_k}{\sigma_k^2 + \lambda} (\boldsymbol{I} \cdot \boldsymbol{v}_k)\boldsymbol{u}_k. \tag{4}$$

In the present case, we have set $M = N = 286$, corresponding to energies from 15 to 300 keV with 1 keV resolution. The regularization parameter λ is determined using the Morozov discrepancy principle, i.e., such that $\|\boldsymbol{AF} - \boldsymbol{I}\|^2/N$ is equal to the mean square data noise (Tikhonov et al. 1995). Equation (4) shows that singular functions $\boldsymbol{u}_k(E)$ with associated eigenvalues $\sigma_k \ll \sqrt{\lambda}$ (which are generally associated with lack of smoothness) are effectively suppressed relative to those (smoother) $\boldsymbol{u}_k(E)$ that are associated with larger values of σ_k; for more details, see Massone et al. (2003).

3. ANALYSIS PROCEDURE

We first obtained the *Reuven Ramaty High Energy Solar Spectroscopic Imager* (*RHESSI*) count rate spectrum for the period 00:30:00–00:30:20 UT during the 2002 July 23 flare. This time interval is near the time of peak hard X-ray flux and corresponds to one of the intervals studied by Holman et al. (2003) in their forward-fitting approach. The corresponding photon spectrum $I(\epsilon)$ was then derived according to the procedure discussed by Kontar et al. (2003). This resulted in a photon spectrum $I(\epsilon)$ in 1 keV bins spanning the range 15–300 keV. Then, using the bremsstrahlung cross section $Q(\epsilon, E)$ due to Haug (1997; his eqs. [4] and [5]), weighted by a factor $Z^2 = 1.44$ to take into account bremsstrahlung on heavy elements, we calculated the corresponding singular values σ_k and vectors $\boldsymbol{v}_k$, $\boldsymbol{u}_k$, and hence, using equation (4), the regularized mean electron spectrum $F(E)$.

We note that obtaining photon spectra at a high level of accuracy depends on knowledge of several instrument-related factors (e.g., pulse pileup and the spectral dependence of grid transmission vs. viewing angle) that are not currently known to this level of accuracy. This remaining few percent uncertainty in $I(\epsilon)$ will affect the precise values of $\bar{F}(E)$ obtained but should not radically affect the essential conclusions of this Letter. Final determination of absolute mean electron spectra $F(E)$ must, however, await a more through understanding of these instrumental effects.

Any valid form of $F(E)$ must, of course, satisfactorily account for the observed photon spectrum. In this Letter, we have set up the problem as "square," i.e., determining electron energies E at 1 keV intervals in the [15, 300] keV range using photon data at the same discrete energies. However, due to noise in the photon data, the quality of the recovered electron spectrum $F(E)$ above ~160 keV was rather poor, and the spectrum was therefore truncated at this value. While such a truncation does not introduce serious errors in the corresponding photon spectrum for sufficiently soft (steep) spectra, the photon spectrum near the peak of the 2002 July 23 event was actually very hard, with a spectral index $\gamma \simeq 3.5$ (Holman et al. 2003). For such a flat spectrum, higher energy ($E > 160$ keV) electrons *do* contribute significantly to the photon spectrum in the observed range, so that an extrapolation of the recovered electron spectrum above $E = 160$ keV is necessary in order to correctly account for the observed photon spectrum (see Johns & Lin 1992).

We here extend the electron spectrum from 160 keV up to 1 MeV by a power law. The errors in the recovered photon spectrum resulting from the neglect of electrons of even higher energies ($E > 1$ MeV) are negligible compared with the data noise. A full treatment of such a spectral extrapolation would calculate the photon spectrum in the range $\epsilon = [15, 160]$ keV produced by the extrapolated part of the electron spectrum (i.e., from electrons with energies 160 keV $< E <$ 1 MeV) and subtract this from the observed data to yield (see Johns & Lin 1992) the photon spectrum produced by the remaining electrons (i.e., those with energies in the range 15 keV $< E <$ 160 keV). The electron spectrum in this range would then be obtained through the "square" regularized inversion algorithm described in § 2. In this Letter, we abbreviate this process somewhat by simply adding the power-law–extrapolated spectrum for $E >$ 160 keV to the [15, 160] keV portion of the regularized spectrum, obtained using equation (4). The differences in the [15, 160] keV electron spectra therefore depend on the differences between the actual electron spectrum above 160 keV and the power-law–extrapolated form. Based on the fidelity of a power-law fit to the data in the range $\epsilon > 160$ keV (Holman et al. 2003), these differences should be small.

This power-law extrapolation process allows us to improve the fit between the data and the reconstructed photon spectrum (determined using the electron spectrum over the entire range 15 keV $< E <$ 1 MeV). The value of the power-law spectral index δ was chosen through optimization of the fit to the observed photon spectrum (see § 4) to be $\delta = 2.45$, which is very close to the value $\delta = 2.48$ found for the energy range greater than 130 keV through the forward-fitting procedure of Holman et al. (2003). However, due to differences between the actual spectrum above 160 keV and the extrapolated power-law form, systematic deviations in the photon spectral fit may (and indeed do) occur.

4. RESULTS

Figure 1 shows the quantity $\bar{n}V\bar{F}(E)$ (in units of electrons cm^{-2} s^{-1} keV^{-1}) for the interval 00:30:00–00:30:20 UT. The ($3\,\sigma$) vertical extents of the error boxes were deduced from

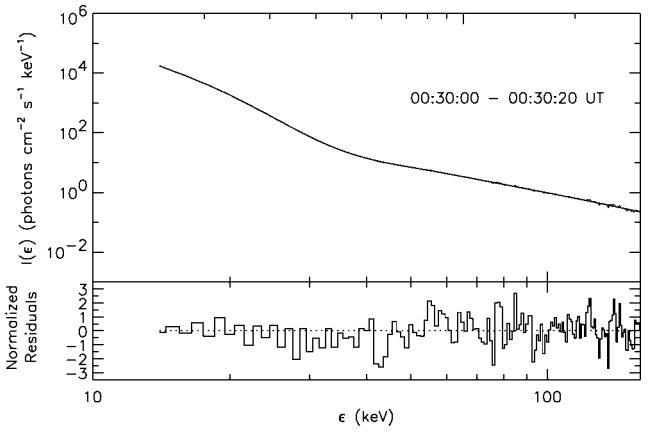

FIG. 2.—*Top panel*: Reconstructed photon spectrum $I(\epsilon)$ for the time interval 00:30:00–00:30:20 UT, compared with the data. *Bottom panel*: Residuals (data-reconstructed spectrum), normalized to the standard deviation in the data at each point.

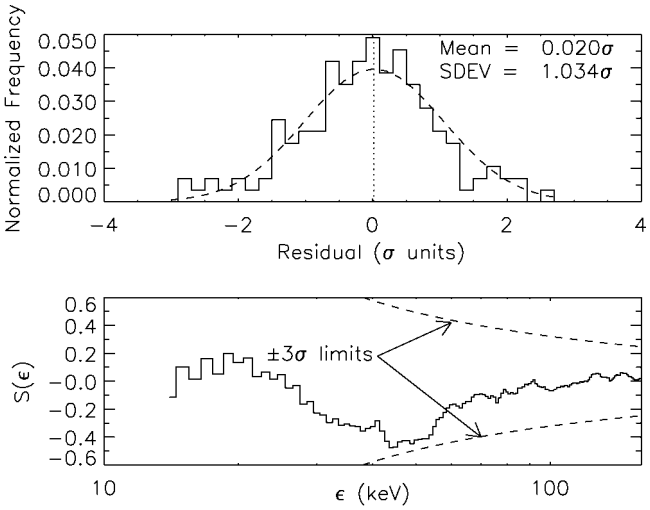

FIG. 3.—*Top panel:* Distribution function for the normalized residuals of Fig. 2. A Gaussian fit, with the mean and standard deviation values indicated, has been superposed. *Bottom panel:* $S(\epsilon)$ (the average residual over the energy range from 15 keV to ϵ; see eq. [5]) as a function of ϵ. The $\pm 3\,\sigma$ limits for a random statistical process are shown for comparison.

repeated inversions using different uniform random realizations of the data set, with the uncertainties in the photon spectrum deduced from the Poisson uncertainties in the instrument count rates in each 1 keV energy channel. [This procedure for determining the uncertainties in the recovered mean source electron spectrum $F(E)$ does not incorporate possible systematic effects (e.g., Smith et al. 2002) in the photon spectra used for the analysis. Therefore, features that appear may reflect, to some degree, such systematic errors rather than real features in the actual $F(E)$. Differentiation between real features and those introduced by systematic effects will improve as our understanding of the latter is improved.]

The spectrum deduced by Holman et al. (2003) based on an isothermal+power-law fit is shown for comparison in Figure 1. The absolute values, and general trends, of the forward-fitted and regularized inverted spectra agree very well over the whole energy range, so that "global" quantities such as energy content, etc., are equally well calculated from either spectrum. However, the regularized spectrum shows significant features (such as a local minimum near 55 keV) that cannot be detected by procedures such as parametric power-law fitting. It also shows the true form of $F(E)$ at low energies without any assumption about thermality or nonthermality of the electron population, far less the usual assumption of *iso*thermality.

The top panel of Figure 2 shows the reconstructed photon spectrum over the photon energy range up to 300 keV, obtained by convoluting the $\bar{n}VF(E)$ spectrum of Figure 1 up to electron energies of 1 MeV with the Haug (1997) bremsstrahlung cross section. The bottom panel of Figure 2 shows the residuals (data minus reconstructed spectrum, normalized to the standard deviation in the photon flux at each energy) over the same energy range.

The top panel of Figure 3 shows the distribution of the sizes of the normalized residuals; they are well fitted by a Gaussian form with a mean of $+0.020\,\sigma$ and a standard deviation of $1.034\,\sigma$. With 146 points (15–160 keV in 1 keV steps) in the distribution, the standard error in the mean is $1.034\,\sigma/\sqrt{146} \simeq 0.086\,\sigma$; hence, the measured offset of the mean from zero is only 0.23 of a standard error and so not significant. However, the pattern of residuals shown in the bottom panel of Figure 2 indicates that merely having a Gaussian distribution of residuals is not a sufficiently stringent test; it is also necessary to consider the distribution of residuals with respect to photon energy ϵ, in order to assess the level of clustering of positive and/or negative residuals in certain energy ranges (e.g., the apparent tendency for the residuals to be consistently negative in the photon energy range from ~25 to 45 keV). We therefore consider the function

$$S(\epsilon) = \frac{1}{N}\sum_{i=1}^{N} r_i, \tag{5}$$

where r_i is the ith normalized residual, corresponding to the photon energy $(14 + i)$ keV, as shown in the bottom panel of Figure 2, and $\epsilon = (14 + N)$ keV is the photon energy corresponding to the Nth residual. The quantity $S(\epsilon)$ is the average (normalized) residual over the photon energy interval [15 keV, ϵ]; if the residuals were randomly distributed, then $S(\epsilon)$ would exhibit a random walk with a standard deviation $\sigma = 1/\sqrt{N}$. We found that varying the spectral index δ of the greater than 160 keV extrapolated electron spectrum $F(E)$ (see § 3) resulted in significantly different forms of $S(\epsilon)$. Many of these forms exhibited deviations from zero greater than $3\,\sigma$. Such forms indicate an unacceptable level of clustering of positive (or negative) residuals and hence a value of δ that can be rejected at the 99% confidence level. The value of δ was chosen to yield the most acceptable behavior of $S(\epsilon)$ (i.e., least maximum deviation from zero), i.e., $\delta = 2.45$.

The bottom panel of Figure 3 shows the actual variation of $S(\epsilon)$ for the residuals shown in Figure 2. $S(\epsilon)$ stays within the $3\,\sigma$ random walk limits over the entire energy range, so that the null hypothesis (of residuals distributed randomly with respect to photon energy) is acceptable. Nevertheless, there is significant evidence of some clustering of residuals [e.g., the systematic decrease in $S(\epsilon)$ from ~25 to 45 keV], which is a subject for future investigation.

We conclude that the form of $\bar{F}(E)$ in Figure 1 yields an acceptable fit to the photon spectrum, with residuals consistent with random data noise. Based on this fidelity in fitting the photon spectrum, we assert that the electron spectral features in Figure 1 are real and therefore carry important information. (While, to the eye, the nearly power-law photon spectra resulting from a single– or double–power-law mean electron

spectrum also look very good, with a small χ^2 [Holman et al. 2003], such apparent fits are very misleading in the case of ill-posed inverse problems [Craig & Brown 1986].) In particular, the dip in $F(E)$ at around 50–60 keV, the significant excess over an isothermal form in the ~30–45 keV range, and the fact that the $F(E)$ spectrum is *increasing* over the energy interval from ~55 to ~60 keV are all significant features at up to the 5 σ level.

5. DISCUSSION

In this Letter, we have shown that the regularized SVD inversion technique (Tikhonov 1963; Piana 1994) can be used rather productively to derive effective mean electron flux spectra [$\bar{F}(E)$; Brown et al. 2003] in solar flares. The spectra thus derived reveal features not accessible with the simple parametric forms usually associated with forward-fitting methods.

The feature in $F(E)$ around 55 keV must indicate an energy characterizing the physics either of the acceleration process or of electron propagation/energy losses. It could indicate the presence of a lower limit to the accelerated electron spectrum, with the shallowing of the $F(E)$ spectral slope between ~30 and 50 keV due to the presence of thermal plasma from a source with a broad temperature distribution (see, e.g., Brown 1974 and Brown & Emslie 1988), with a steadily declining emission measure over a range of temperature consistent with the range of electron energies involved, viz., 10 keV $\lesssim kT \lesssim$ 50 keV, much larger than the dominant, purely isothermal component at $kT \simeq 3$ keV found by Holman et al. (2003).

If the acceleration were purely stochastic in character, one would expect a scale-free acceleration spectrum (i.e., a pure power law). Attributing the feature in $\bar{F}(E)$ to the accelerator would thus require either that the stochastic process have a threshold energy or that acceleration be by large-scale electric fields with a minimum associated potential drop. As far as propagation effects are concerned, it should be remarked that the energy of this feature is very close to the value of the quantity E_* found by Kontar et al. (2003) in their forward-fitting analysis of the hard X-ray photon spectrum for this event. In that analysis, E_* represents the energy required to penetrate to the weakly ionized chromospheric layers of the flare, and it is therefore not unexpected that the $F(E)$ spectrum would show interesting features in the vicinity of this energy (Kontar, Brown, & McArthur 2002; Brown et al. 2003).

Such features, and their significance for electron acceleration and propagation in solar flares, will be addressed in future work. The key point for now is that, unlike forward-fitting techniques that utilize only a few parameters (e.g., the power-law spectral index), the regularized inversion technique utilized here is capable of revealing such interesting features and their evolution with time. In future papers, the sensitivity of such features to the exact form of the bremsstrahlung cross section used, and the evolution of such features throughout this (and other) events, will be discussed and evaluated.

This work was supported by NASA's Office of Space Science through grant NAS5-98033, by PPARC *RHESSI* Mission and Visitor Grants, and by a Collaboration Grant from the Royal Society. We thank Hugh Hudson and Bob Lin for their critical commentary throughout the evolution of this work and the entire *RHESSI* team for the hardware and software development that made this analysis possible.

REFERENCES

Bertero, M., de Mol, C., & Pike, E. R. 1988, Inverse Problems, 4, 573
Brown, J. C. 1971, Sol. Phys., 18, 489
———. 1974, in IAU Symp. 57, Coronal Distrurbances, ed. G. A. Newkirk Jr. (Dordrecht: Kluwer), 395
Brown, J. C., & Emslie, A. G. 1988, ApJ, 331, 554
Brown, J. C., Emslie, A. G., & Kontar, E. P. 2003, ApJ, 595, L115
Craig, I. J. D., & Brown, J. C. 1986, Inverse Problems in Astronomy (Bristol: A. Hilger)
Golub, G. H., & Van Loan, C. F. 1933, Matrix Computation (Baltimore: Johns Hopkins Univ. Press)
Haug, E. 1997, A&A, 326, 417
Holman, G. D., Sui, L., Schwartz, R. A., & Emslie, A. G. 2003, ApJ, 595, L97
Johns, C., & Lin, R. P. 1992, Sol. Phys., 137, 121
Kontar, E. P., Brown, J. C., & McArthur, G. K. 2002, Sol. Phys., 210, 419
Kontar, E. P., Brown, J. C., Emslie, A. G., Schwartz, R. A., Smith, D. M., & Alexander, R. C. 2003, ApJ, 595, L123
Massone, A. M., Piana, M., Conway, A. J., & Eves, B. 2003, A&A, in press
Piana, M. 1994, A&A, 288, 949
Piana, M., & Brown, J. C. 1998, A&AS, 132, 291
Smith, D. M., et al. 2002, Sol. Phys., 210, 33
Thompson, A. M., Brown, J. C., Craig, I. J. D., & Fulber, C. 1992, A&A, 265, 278
Tikhonov, A. N. 1963, Soviet Math. Dokl., 4, 1035
Tikhonov, A. N., Goncharsky, A. V., Stepanov, V. V., & Yagola, A. G. 1995, Numerical Methods for the Solution of Ill-posed Problems (Dordrecht: Kluwer)